

## Bent Optical Waveguide With Lossy Jacket

By D. MARCUSE

(Manuscript received December 20, 1973)

*The influence of a lossy jacket on the curvature losses of a bent optical waveguide is studied for the special case of the TE modes of a slab waveguide. This paper presents an approximate theory of curvature losses of the TE modes of dielectric slabs that can be used to obtain numerical answers with the help of a computer. We conclude that the presence of a jacket can increase the curvature losses very substantially. A jacket whose refractive index is larger than that of the waveguide cladding is most effective in increasing cladding losses. It is advisable to keep a jacket at a safe distance from the waveguide core.*

### I. INTRODUCTION

To avoid crosstalk between adjacent fibers in a cable and also to suppress unwanted cladding modes, optical fibers for communication purposes need lossy jackets.<sup>1</sup> Each fiber thus consists of a core of refractive index  $n_1$  and a cladding with index  $n_2$ . Since core and cladding are made of low-loss materials, we consider  $n_1$  and  $n_2$  real constants. The refractive index of the lossy jacket is considered complex:

$$n_3 = n_{3r} - in_{3i}. \quad (1)$$

The negative sign is necessary since we use the time dependence

$$e^{i\omega t} \quad (2)$$

for the optical waves.

The guided-mode fields decrease in intensity exponentially with increasing distance from the fiber core. At the boundary between the cladding and the lossy jacket, the intensity of the modes should decrease to insignificant values. If the cladding is too thin, so that the modes arrive at the cladding-jacket boundary with appreciable field intensities, considerable amounts of power would be dissipated in the lossy jacket, resulting in intolerably high waveguide losses. The de-

signer must provide for a cladding of sufficient thickness to keep the fiber losses low.

So far, we have considered a fiber that is perfectly straight. However, an advantage of optical fiber systems is that light transmission is maintained as the fiber is curved. Since curvature of the fiber axis distorts the shape of the guided modes,<sup>2</sup> it is necessary to study the effect of the lossy jacket in the presence of fiber curvature. A curved fiber radiates a certain amount of power even if its cladding extends infinitely far from the core.<sup>2,3</sup> The amount of radiated power is modified by the presence of the lossy jacket.

It is the purpose of this paper to investigate the influence of the lossy jacket on the curvature losses of optical waveguides. Because of the complexity of the problem, we use the TE modes of the symmetric slab waveguide as a model.

The following sections are devoted to the derivation of the theory. Readers not interested in the theoretical details are advised to turn to Section VI, on numerical examples.

## II. OUTLINE OF THE METHOD OF SOLUTION

A curved slab waveguide with lossy jacket is schematically shown in Fig. 1. The core with refractive index  $n_1$  has the full width  $2d$ . The center line of the core is curved with radius of curvature  $R$ . The cladding with index  $n_2$  has the thickness  $D - d$ . The refractive index of the jacket is assumed to be a complex quantity. A straightforward solution of this problem would involve writing down solutions of Maxwell's equations in the five different regions of the structure. These solutions can be expressed in terms of cylinder functions. The waveguide modes are obtained by joining the solutions in the different regions with the help of boundary conditions. This straightforward procedure is not practical for the determination of the fiber losses. To understand the difficulty, we must consider that the cylinder functions, expressing the solutions of Maxwell's equations, have very large order numbers and arguments that are of the same order of magnitude as the order numbers. The problem consists in finding the order number as a solution of an eigenvalue problem. Since we expect to compute the waveguide losses, the order of the Bessel functions must be a complex quantity. We are thus faced with solving a determinantal equation whose elements are cylinder functions of very large complex order. Cylinder functions of this type cannot be computed with the help of power series expansions. The functions must be obtained from approximate asymptotic expressions. The solution of the complex

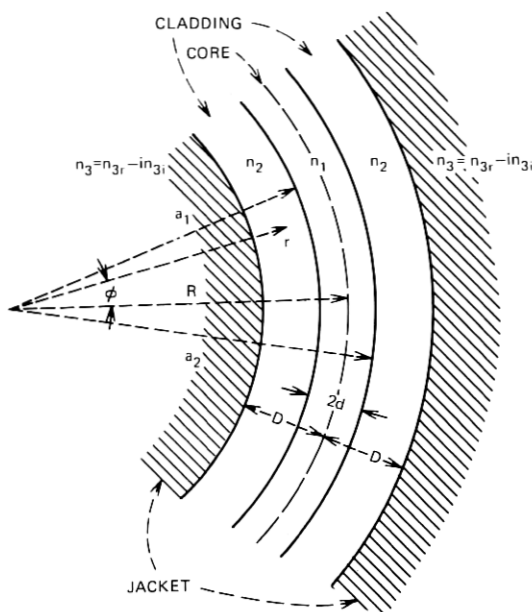


Fig. 1—Schematic of the bent slab waveguide with lossy jacket. The  $z$ -axis is directed normal to the plane of the figure.

transcendental eigenvalue equation thus not only is a difficult numerical task, but also may be expected to yield poor accuracy since we expect the imaginary part of the eigenvalue (the order number of the cylinder functions) to be small so that it could be obtained with high accuracy only if the functions themselves are known to high precision.

Since the straightforward approach seems to present an almost insurmountable obstacle, we use a different approach. Instead of solving the problem sketched in Fig. 1, we begin by solving the simpler problem that results if we let  $D \rightarrow \infty$ . The exact solution of the bent slab with infinite cladding thickness still results in a complex eigenvalue, since radiation losses occur. However, we are not interested in computing the radiation losses at this point and modify the eigenvalue equation so that its imaginary part is neglected. We are now left with a relatively simple eigenvalue problem. It is still necessary to compute cylinder functions of large order and argument. But since only a real eigenvalue is computed with the help of real cylinder functions, the usual asymptotic approximations of the cylinder functions can be used.

The next step of our approximate procedure consists in determining the reflection and transmission coefficients of a cylindrical wave im-

pinging on a cylindrical dielectric interface. Once this problem is solved, we apply its solutions to the evanescent field tail of the guided wave in the cladding. In this way, we obtain approximate field expressions for the field reaching into the lossy jacket. It is now a simple matter to calculate the amount of power flowing from the guided mode into the lossy jacket and to use it to determine the waveguide losses.

In the following sections, we outline the mathematical details of our approximate procedure. The only difficulty encountered consists in producing the cylinder functions of large order and, at least inside the lossy jacket, of complex argument.

### III. BENT SLAB WAVEGUIDE WITH INFINITELY WIDE CLADDING

We are interested in the TE modes of the curved slab. Using the coordinates indicated in Fig. 1, we can express the  $z$  component of the electric field in the three regions as

$$E_z = \begin{cases} AJ_\nu(n_2kr)e^{-i\nu\phi} & 0 < r < a_1 \\ [BJ_\nu(n_1kr) + CN_\nu(n_1kr)]e^{-i\nu\phi} & a_1 < r < a_2 \\ FH_\nu^{(2)}(n_2kr)e^{-i\nu\phi} & a_2 < r < \infty. \end{cases} \quad (3)$$

The  $z$  coordinate is directed perpendicular to the plane of the figure. The Bessel and Neumann functions of order  $\nu$  are  $J_\nu$  and  $N_\nu$ . The free space propagation constant is defined as

$$k = \frac{2\pi}{\lambda} = \omega\sqrt{\epsilon_0\mu_0}. \quad (4)$$

The  $r$  and  $\phi$  components of the magnetic fields are obtained from the  $E_z$  component by differentiation.<sup>4</sup>

$$H_r = \frac{i}{\omega\mu_0} \frac{1}{r} \frac{\partial E_z}{\partial \phi} = \frac{1}{\omega\mu_0} \frac{\nu}{r} E_z \quad (5)$$

$$H_\phi = \frac{-i}{\omega\mu_0} \frac{\partial E_z}{\partial r}. \quad (6)$$

The remaining field components  $E_r$ ,  $E_\phi$ , and  $H_z$  vanish. Since the waves travel along the curved slab in  $\phi$  direction, we can define the propagation constant of the guided mode

$$\beta = \frac{\nu}{R}. \quad (7)$$

The requirement of continuity of the  $E_z$  and  $H_\phi$  components at the core boundaries  $r = a_1$  and  $r = a_2$  lead to the determination of the

amplitude coefficients

$$A = \frac{n_1 J_\nu(x_{11}) N'_\nu(x_{11}) - n_1 J'_\nu(x_{11}) N_\nu(x_{11})}{n_1 J_\nu(x_{21}) N'_\nu(x_{11}) - n_2 J'_\nu(x_{21}) N_\nu(x_{11})} B, \quad (8)$$

$$C = - \frac{n_1 J_\nu(x_{21}) J'_\nu(x_{11}) - n_2 J'_\nu(x_{21}) J_\nu(x_{11})}{n_1 J_\nu(x_{21}) N'_\nu(x_{11}) - n_2 J'_\nu(x_{21}) N_\nu(x_{11})} B, \quad (9)$$

and

$$F = \frac{1}{H_\nu^{(2)}(x_{22})} [BJ_\nu(x_{12}) + CN_\nu(x_{12})]. \quad (10)$$

The definition

$$x_{ij} = n_i k a_j \quad (11)$$

was used. The prime indicates the derivative of the functions with respect to the argument.

The Bessel and Neumann functions are real. The Hankel function of the second kind appearing in (3) and (10) is complex,

$$H_\nu^{(2)} = J_\nu - iN_\nu. \quad (12)$$

Because of the complex value of  $H_\nu^{(2)}$ , the eigenvalue equation (that results from the requirement that the determinant of the equation system for the determination of  $A$ ,  $B$ ,  $C$ , and  $F$  vanish) is itself complex, leading to complex solutions for  $\nu$ . However, for well-guided modes we have

$$\nu > n_2 k a_2 \gg 1. \quad (13)$$

The inequality (13) results, in turn, in

$$|J_\nu(x_{22})| \ll |N_\nu(x_{22})|. \quad (14)$$

The Hankel function is thus predominantly imaginary with a very small real part. By replacing the Hankel function with the approximation

$$H_\nu^{(2)} = -iN_\nu \quad (15)$$

in (3) and (10), we obtain the real eigenvalue equation

$$\begin{aligned} & [n_2 J_\nu(x_{11}) J'_\nu(x_{21}) - n_1 J_\nu(x_{21}) J'_\nu(x_{11})] \\ & \times [n_1 N_\nu(x_{22}) N'_\nu(x_{12}) - n_2 N'_\nu(x_{22}) N_\nu(x_{12})] \\ & + [n_1 J_\nu(x_{21}) N'_\nu(x_{11}) - n_2 J'_\nu(x_{21}) N_\nu(x_{11})] \\ & \times [n_1 J'_\nu(x_{12}) N_\nu(x_{22}) - n_2 J_\nu(x_{12}) N'_\nu(x_{22})] = 0. \end{aligned} \quad (16)$$

This eigenvalue equation has real solutions of  $\nu$  ignoring radiation losses caused by waveguide curvature. However, the mode problem that we have formulated describes the distorted fields in the curved

waveguide accurately. The curvature losses are obtained later by accounting for the amount of power that is lost in the form of radiation.

The power carried by the modes can be expressed as

$$P = \frac{1}{4\omega\mu_0} \left\{ A^2 \left[ x \left( J_{\nu+1} \frac{\partial J_\nu}{\partial \nu} - J_\nu \frac{\partial J_{\nu+1}}{\partial \nu} \right) + J_\nu^2 \right]_0^{x_{21}} \right. \\ + B^2 \left[ x \left( J_{\nu+1} \frac{\partial J_\nu}{\partial \nu} - J_\nu \frac{\partial J_{\nu+1}}{\partial \nu} \right) + J_\nu^2 \right]_{x_{11}}^{x_{21}} \\ + 2BC \left[ x \left( J_{\nu+1} \frac{\partial N_\nu}{\partial \nu} - N_\nu \frac{\partial J_{\nu+1}}{\partial \nu} \right) + J_\nu N_\nu \right]_{x_{11}}^{x_{12}} \\ + C^2 \left[ x \left( N_{\nu+1} \frac{\partial N_\nu}{\partial \nu} - N_\nu \frac{\partial N_{\nu+1}}{\partial \nu} \right) + N_\nu^2 \right]_{x_{11}}^{x_{12}} \\ \left. + |F|^2 \left[ x \left( N_{\nu+1} \frac{\partial N_\nu}{\partial \nu} - N_\nu \frac{\partial N_{\nu+1}}{\partial \nu} \right) + N_\nu^2 \right]_{x_{22}}^\infty \right\}. \quad (17)$$

The notation  $[ \quad ]_{x_1}^{x_2}$  indicates that the value of the bracket evaluated at  $x_1$  must be subtracted from the expression evaluated at  $x_2$ . Since the ratios of the amplitude coefficients are real quantities,  $A$ ,  $B$ , and  $C$  are assumed real. However, with approximation (15),  $F$  becomes imaginary. The contributions of the lower limit 0 of the first bracket and of the upper limit  $\infty$  of the last bracket may be neglected since the fields decrease rapidly with increasing distance from the waveguide core.

#### IV. REFLECTION AND TRANSMISSION OF A WAVE AT A CYLINDRICAL INTERFACE

Our solution of the mode problem of the bent slab waveguide ignored radiation losses caused by the curvature and losses resulting from the presence of the lossy jacket. We calculate these losses by accounting for the outflow of power from the curved waveguide. To obtain expressions for the power outflow, we study the problem of a cylindrical wave that is impinging on a cylindrical interface between two dielectric media.

Ignoring, for the moment, the presence of the waveguide core and the jacket region that contains the center of curvature, we consider a cylindrical wave in the region to the left of the interface between the media with refractive indices  $n_2$  and  $n_3$ ,

$$E_z = [GH_\nu^{(2)}(n_2kr) + IH_\nu^{(1)}(n_3kr)]e^{-i\nu\phi} \quad R + d < r < R + D. \quad (18)$$

According to time dependence (2), the Hankel function of the second kind describes the incident cylindrical wave, while the Hankel function

of the first kind belongs to the reflected wave. Inside the jacket we have a transmitted wave

$$E_z = KH_\nu^{(2)}(n_3kr)e^{-i\nu\phi} \quad r > R + D. \quad (19)$$

The corresponding magnetic field components follow again from (5) and (6). Continuity of the  $E_z$  and  $H_\phi$  components is achieved if the following relations hold between the three amplitude coefficients:

$$I = \frac{n_3H_\nu^{(2)}(y_2)H_\nu^{(2)'}(y_3) - n_2H_\nu^{(2)'}(y_2)H_\nu^{(2)}(y_3)}{n_2H_\nu^{(1)'}(y_2)H_\nu^{(2)}(y_3) - n_3H_\nu^{(2)'}(y_3)H_\nu^{(1)}(y_2)} G \quad (20)$$

and

$$K = \frac{n_2H_\nu^{(1)'}(y_2)H_\nu^{(2)}(y_2) - n_2H_\nu^{(1)}(y_2)H_\nu^{(2)'}(y_2)}{n_2H_\nu^{(1)'}(y_2)H_\nu^{(2)}(y_3) - n_3H_\nu^{(1)}(y_2)H_\nu^{(2)'}(y_3)} G, \quad (21)$$

with

$$y_i = n_i k(R + D). \quad (22)$$

It remains to relate the amplitude  $G$  to the amplitude  $F$  of the evanescent field tail of the guided mode in the curved slab. Our treatment is, of course, not exact, since multiple reflections of the wave between core and jacket are ignored. However, if the refractive index differences remain small, multiple reflections are unimportant. Furthermore, the field intensity decays exponentially with increasing distance from the waveguide core. The incident wave  $GH_\nu^{(2)}(n_2kr)$  is, thus, an evanescent wave in most cases so that the effect of the core cladding boundary on this wave is only very slight. Whether the incident wave is an evanescent or a propagating wave depends on the distance between core and jacket. If this distance is small, the guided mode field behaves predominantly as an evanescent wave. If the distance between core and jacket is large, the evanescent wave has converted itself to a traveling wave before the jacket is reached. Our approximate procedure works in either case for most cases of practical interest.

To obtain the relation between the amplitude  $G$  and the amplitude  $F$  of the guided wave, we consider the field in the immediate vicinity of the core boundary and equate the fields (3) and (18)

$$FH_\nu^{(2)}(n_2kr) = GH_\nu^{(2)}(n_2kr) + IH_\nu^{(1)}(n_2kr). \quad (23)$$

It was explained earlier that we may approximate the Hankel function of the second kind by (15). Likewise, we use the approximation

$$H_\nu^{(1)} = iN_\nu. \quad (24)$$

Using (15) and (24), we obtain from (23)

$$G = \frac{F}{1 - \frac{I}{G}}. \quad (25)$$

The ratio  $I/G$  is given by (20). We thus have determined the amplitude of the wave that is incident on the jacket (at least approximately) and can now compute the amount of power that is carried into the jacket.

## V. CALCULATION OF THE LOSSES

The amount of power outflow in  $r$  direction per unit length along the waveguide axis (and also per unit length in  $z$  direction) is given by the  $r$  component of the Poynting vector

$$S_r = -\frac{1}{2} \operatorname{Re} \{E_z H_\phi^*\}. \quad (26)$$

If we denote by  $\alpha$  the amplitude attenuation coefficient of the guided wave, we obtain the power attenuation coefficient  $2\alpha$  from the relation

$$2\alpha = \frac{S_r}{P}. \quad (27)$$

This relation holds since  $P$  is by definition the amount of power carried by the guided mode per unit length (in  $z$  direction). Using (6), (19), and (26) we obtain

$$2\alpha = \sqrt{\frac{\epsilon_0}{\mu_0}} \frac{|K|^2}{2P} \operatorname{Im} \{n_3^* H_\nu^{(2)}(y_3) H_\nu^{(2)*}(y_3)\}. \quad (28)$$

The asterisk indicates complex conjugation and  $\operatorname{Im} ( )$  designates that the imaginary part of the complex expression in brackets is to be taken. The argument  $y_3$  is defined by (22).

A small amount of power also flows into the jacket on the other side of the waveguide, the side facing the center of curvature. However, for reasonably strongly curved guides, this power outflow is orders of magnitude smaller than the power outflow included in (28) so that we may safely neglect it.

The solution of the loss problem is now reduced to a determination of the cylinder functions appearing in our equations. We evaluate (28) by using (8) through (10), (17), (21), and (25). The order of the cylinder functions is determined as a solution of the eigenvalue equa-

tion (16). As stated earlier, our method has the advantage that no complex eigenvalue equation need be solved. Owing to the difficulty of computing accurate values for the cylinder functions of large complex order and large complex argument, a direct determination of the losses with the help of the complex eigenvalue equation is hard to achieve. Our method is straightforward in principle. We only face the computational difficulty of determining the cylinder functions of large real order and, at least for some functions, of large complex argument. However, our present method does not require knowledge of these functions to extreme accuracy.

In two limiting cases, the attenuation formulas for the curved slab waveguide are known. For a straight slab with lossy jacket, we use eq. (10.3-14), p. 420, of Ref. 4.

$$2\alpha = \frac{8\kappa^2\gamma^3 \operatorname{Im}(\rho)e^{-2\gamma(D-d)}}{\beta(1 + \gamma d)(\kappa^2 + \gamma^2)|\gamma + \rho|^2} \quad (29)$$

with

$$\kappa^2 = n_1^2 k^2 - \beta^2, \quad (30)$$

$$\gamma^2 = \beta^2 - n_2^2 k^2, \quad (31)$$

and

$$\rho^2 = \beta^2 - n_3^2 k^2. \quad (32)$$

The propagation constant  $\beta$  is obtained as a solution of the eigenvalue equation

$$\tan \kappa d = \frac{\gamma}{\kappa} \quad (33)$$

for even modes and from

$$\tan \kappa d = -\frac{\kappa}{\gamma} \quad (34)$$

for odd modes.

For a curved slab without lossy jacket but infinitely wide cladding, eq. (9.6-27), p. 404, of Ref. 4 is available,

$$2\alpha = \frac{\kappa^2 \gamma^2}{\beta(1 + \gamma d)(\kappa^2 + \gamma^2)} e^{2\gamma d} \exp \left\{ -\frac{2}{3} \frac{\gamma^3}{\beta^2} R \right\}. \quad (35)$$

If we use the eigenvalue  $\beta$  obtained from (33) or (34), we obtain good results only for single mode guides or for very large radii of curvature. Better agreement with numerical evaluations of (28) is obtained if we use solutions of the eigenvalue equation (16) and calculate  $\beta$  with the help of (7) and the other parameters from (30) and (31).

## VI. NUMERICAL EXAMPLES

The principal problem of evaluating the formulas of our theory consists in generating the Bessel function of large real order and large (sometimes) complex argument. The Hankel functions can be expressed in terms of Bessel and Neumann functions. These latter functions are approximated by using the asymptotic formulas (9.3.7) through (9.3.17) on p. 366 of Ref. 5 and eqs. (9.3.23) and (9.3.24) on p. 367 of the same reference. It is not stated clearly in any reference book on Bessel functions that these asymptotic formulas are valid for complex arguments. [This statement refers to the functions given by (9.3.7) through (9.3.17).] However, the first terms of these expressions can easily be derived either by using the integral representation of Bessel and Neumann functions and the method of steepest descent or [for  $J_\nu(x)$  with  $\nu > x$ ] by using approximate solutions obtained directly from the differential equation. Either method clearly holds also for complex arguments. It may be that the convergence behavior and the error estimates available for real arguments may not apply to

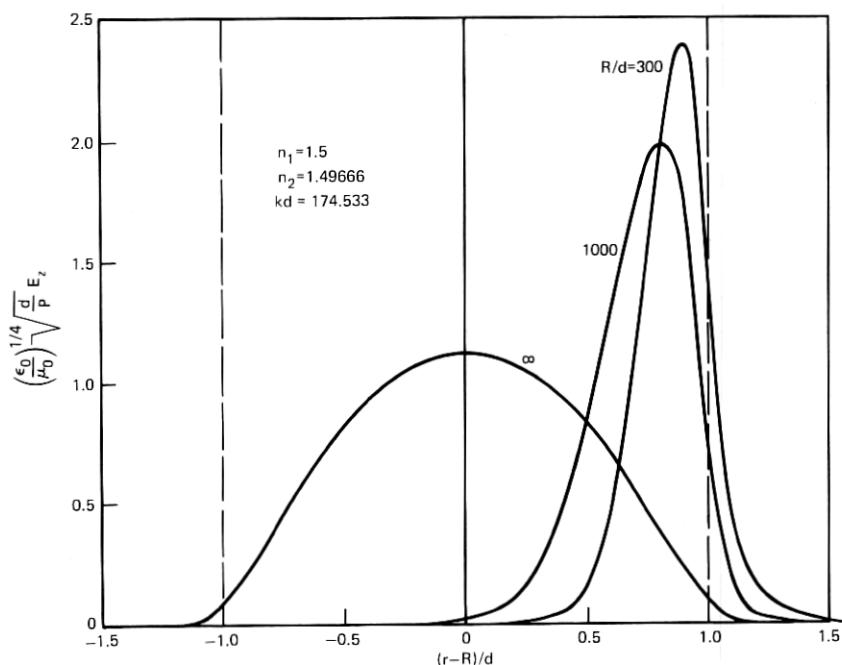


Fig. 2a—Normalized  $E_z$  component of the first guided mode for different radii of curvature. The refractive indices are  $n_1 = 1.5$ ,  $n_2 = 1.49666$ ,  $kd = 174.533$ .

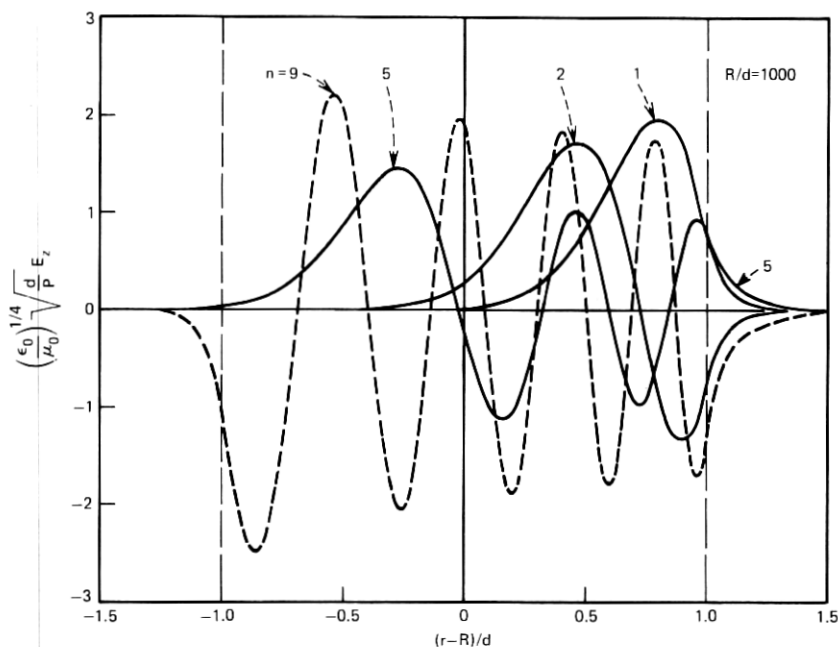


Fig. 2b—Distribution of the electric field for four guided modes,  $n = 1, 2, 5$ , and  $9$  for  $R/d = 1000$ .

complex arguments, but at least the first terms of the asymptotic formulas can be justified for functions with complex argument. For this reason, these formulas were used even if the argument of the cylinder functions is complex. This procedure appears even more valid when we consider that in all cases of practical interest the phase angle of the complex argument remains very small.

The derivatives with respect to the order number were generated by taking the derivatives of the asymptotic formulas. Our method of generating the necessary cylinder functions seems justified by the excellent agreement that was obtained with formulas (29) and (35) in all instances where such agreement could be tested.

Since the arguments of the cylinder functions are of the form  $nkr$ , there are practical limits to the size of the radius of curvature of the waveguide axis. For ratios of  $R/d$  in excess of 1000, exponent overflow was encountered in the numerical calculations so that the limiting case of a straight slab could not be approached very closely.

The distortion of the field distribution caused by waveguide curvature is dramatically evident from the curves of Figs. 2(a) and 2(b).

Figure 2(a) shows the shape of the normalized  $E_z$  component of the lowest order mode, labeled  $n = 1$ , for several values of  $R/d$ . The curve for  $R/d = \infty$  was obtained from eqs. (8.3-9), (8.3-12), and (8.3-18) of Ref. 4. It is apparent that the core cladding boundary on the side facing the center of curvature does not contribute to guiding the lowest-order mode in case of sharp bends. It is also evident that substantial mode conversion must result if a curved waveguide section is joined to a straight waveguide without tapering the curvature. Finally, we see from the figure that the field is forced far deeper into the cladding region by the waveguide curvature so that it tends to interact more strongly with the lossy jacket.

Figure 2(b) shows the distribution of the  $E_z$  fields for several modes. Both figures were drawn for the following parameters:  $n_1 = 1.5$ ,  $n_2 = 1.49666$ ,  $kd = 174.533$ . The important  $V$  parameter defined by

$$V = \sqrt{n_1^2 - n_2^2}kd \quad (36)$$

assumes the value  $V = 17.46$ . The straight slab is thus able to support 11 TE modes. Figure 2(b) shows plots for the modes  $n = 1, 2, 5$ , and 9. We see that the higher-order modes occupy more of the available space inside the waveguide core. The period of oscillation becomes shorter toward the side of the core opposite the center of curvature. However, the field amplitudes are largest on the side nearest the center of curvature.

With regard to the normalization used for the electric field component,

$$\left(\frac{\epsilon_0}{\mu_0}\right)^{1/2} \sqrt{\frac{d}{P}} E_z, \quad (37)$$

we must remember that the parameter  $P$  stands for the power carried by the slab waveguide per unit length (in  $z$  direction).

All numerical examples discussed (with the exception of Fig. 12) are based on the waveguide parameters given above. The propagation constants  $\beta$  obtained from (16) and (7) are listed in Table I for all TE modes that can be supported by the guide for  $R/d = 300, 1000$ , and  $\infty$ . The values for  $R/d = \infty$  were obtained from the eigenvalue equations (33) and (34) for even and odd TE modes of the straight slab waveguide. The table shows that the number of guided modes decreases as the curvature of the guide increases.

Figure 3 shows the normalized loss coefficient  $2\alpha d$  as a function of  $d/R$  for several modes of a slab without jacket. The horizontal dotted lines appearing in this and all subsequent figures indicate the level of 1 dB/km and 10 dB/km loss for a guide with the slab half width

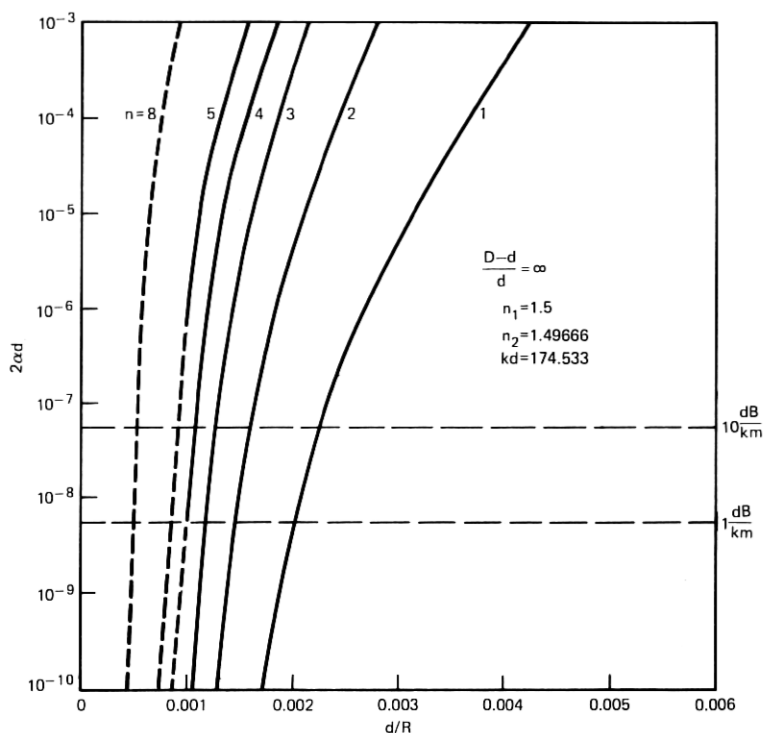


Fig. 3—Curvature losses of a slab with infinitely thick jacket as a function of the inverse radius of curvature for several TE modes. The refractive indices are  $n_1 = 1.5$ ,  $n_2 = 1.49666$ ,  $kd = 174.533$ .

Table I—Values of the normalized propagation constant  $\beta_n d$  for all the TE modes of a curved slab ( $n_1 = 1.5$ ,  $n_2 = 1.49666$ ,  $kd = 174.533$ )

$n$	$\beta_n d$		
	$R/d = 300$	$R/d = 1000$	$R/d = \infty$
1	262.461	261.958	261.795
2	262.270	261.870	261.783
3	262.111	261.797	261.762
4	261.840	261.734	261.732
5	261.498	261.676	261.694
6		261.621	261.648
7		261.569	261.594
8		261.513	261.532
9		261.436	261.463
10		261.381	261.386
11		261.224	261.303

$d = 25 \text{ } \mu\text{m}$ . It is apparent how very strongly the curvature losses depend on the radius of curvature of the waveguide axis. The losses in decibels are obtained by dividing the numerical values, that are read off the vertical axis of the figure, by the slab half width  $d$  and multiplying by 4.34 (to convert the result to decibels).

For a comparison with formula (35), we state that the loss value of the lowest-order mode for  $d/R = 0.001$  is  $2\alpha d = 3.41 \times 10^{-19}$  as computed with the help of the theory presented in this paper. From Table I we find for  $n = 1$ ,  $\beta_1 d = 261.958$ , so that from (31) we obtain  $\gamma d = 19.695$ . If we try to compute  $\kappa^2$  from (30) we find a negative value. Therefore, we use the far-from-cutoff approximation  $\kappa d = \pi/2$ . Using these values in (35), we find  $2\alpha d = 3.37 \times 10^{-19}$  in excellent agreement with the value obtained from our theory. For the high loss values appearing in Fig. 3, the agreement is not as good.

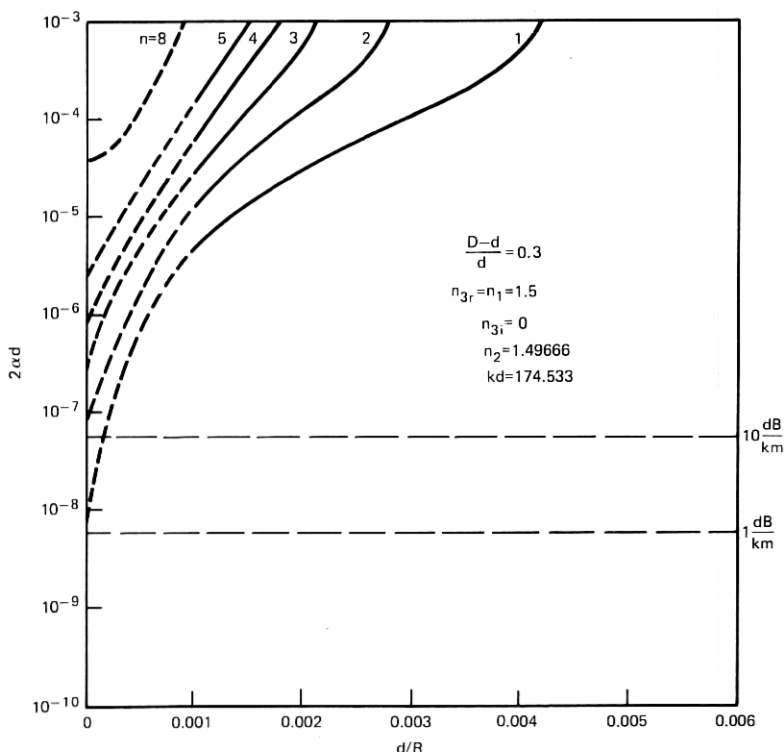


Fig. 4—Curvature losses in the presence of a lossless jacket. The normalized cladding thickness is  $(D - d)/d = 0.3$  and the refractive indices are  $n_1 = 1.5$ ,  $n_2 = 1.49666$ ,  $kd = 174.533$ ,  $n_{3r} = n_1$ ,  $n_{3i} = 0$ .

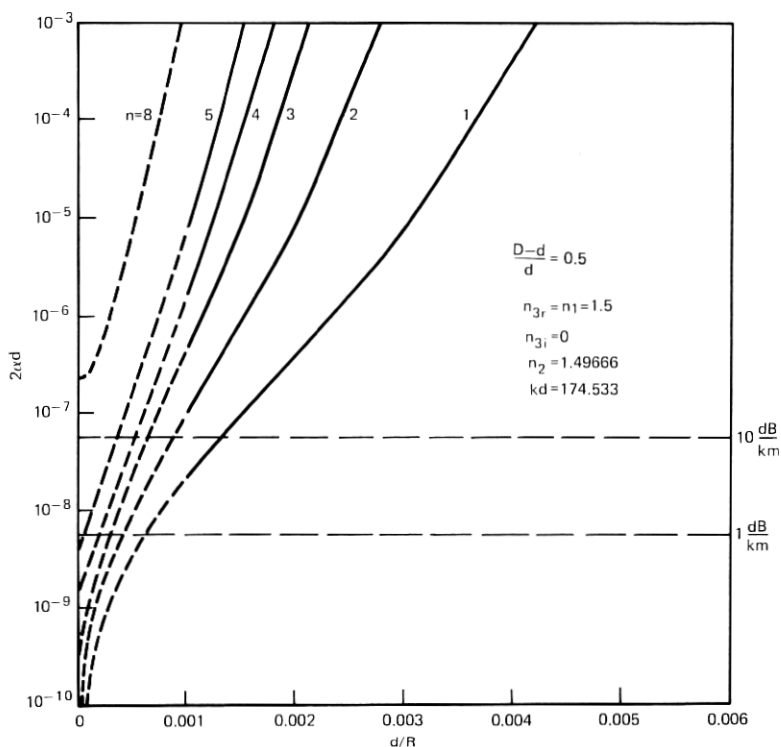


Fig. 5—Curvature losses in the presence of a lossless jacket. The normalized cladding thickness is  $(D - d)/d = 0.5$  and the refractive indices are  $n_1 = 1.5$ ,  $n_2 = 1.49666$ ,  $kd = 174.533$ ,  $n_{3r} = n_1$ ,  $n_{3i} = 0$ .

To gain insight into the effect that the jacket has on the curvature losses, we have plotted the loss values that result if we use a lossless jacket whose refractive index equals that of the waveguide core. Even though the lossless jacket does not dissipate power, it causes the portion of the evanescent field tail reaching the jacket to turn into a propagating wave and thus to radiate away. Figures 4 through 6 show the curvature losses in the presence of the "high-index" jacket as a function of  $d/R$  for several modes and for different values of the relative cladding thickness  $(D - d)/d$ . Comparison of Figs. 3 and 4 shows clearly the dramatic increase in the curvature losses for a thin cladding with  $(D - d)/d = 0.3$ . As the cladding becomes thicker, the influence of the jacket decreases, as seen in Fig. 5. The upper parts of the curves in Fig. 6 already coincide with the curves of Fig. 3 for an infinitely thick cladding. In this case, the field detaches itself from the guide

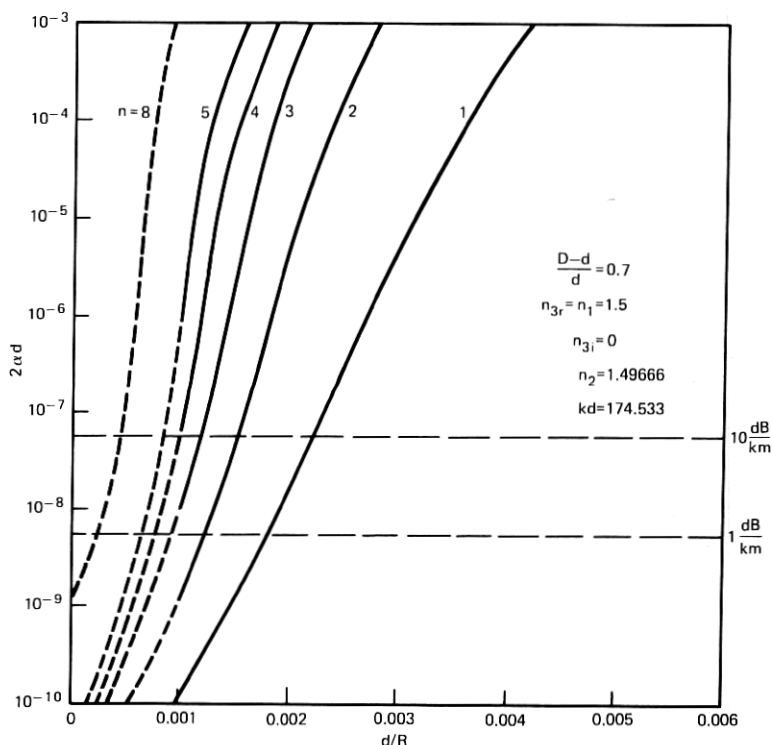


Fig. 6—Curvature losses in the presence of a lossless jacket. The normalized cladding thickness is  $(D - d)/d = 0.7$  and the refractive indices are  $n_1 = 1.5$ ,  $n_2 = 1.49666$ ,  $kd = 174.533$ ,  $n_{3r} = n_1$ ,  $n_{3i} = 0$ .

inside the cladding so that the jacket no longer converts an evanescent field tail into a radiation field, but simply modifies the radiation field in an almost imperceptible way. These curves show that it is very necessary to maintain the "high-index jacket" at a sufficient distance from the waveguide core.

The dotted lines in these and all following figures are estimated curves. We pointed out that the computer program fails to function for very large values of  $R/d$ . The solid lines are the results of the numerical evaluation of our theory. The end points of the dotted curves at  $d/R = 0$  were computed from (29). The region between  $d/R = 0$  and  $d/R = 0.001$  was bridged by the estimated dotted lines.

The curves for mode 8 shown in these and subsequent figures have a special meaning. We want to use our slab model to gain information about round fibers. If we consider a fiber with core radius  $a = d$  and

the same refractive indices used for the slab, the total number  $M$  of fiber modes is proportional to the square of the total number  $N$  of slab modes,  $M = KN^2$ . It is instructive to consider fibers capable of transmitting at least half their total number of guided modes. The corresponding number of slab modes is  $N' = N/\sqrt{2}$ . With our numerical values we have a slab supporting  $N = 11$  modes.  $N' = 11/\sqrt{2} = 8$  is thus the mode number that corresponds to half the total number of fiber modes. If the losses of mode  $n = 8$  are just tolerable, but all higher-order modes suffer too much loss, we know that we have found operating conditions that would cause half the total number of fiber modes to be lost. For this reason, we have included mode  $n = 8$  in our figures to be able to estimate the conditions that would allow half the fiber modes to be transmitted. Figure 4 shows that only a very small number of modes can propagate with low losses in a fiber whose

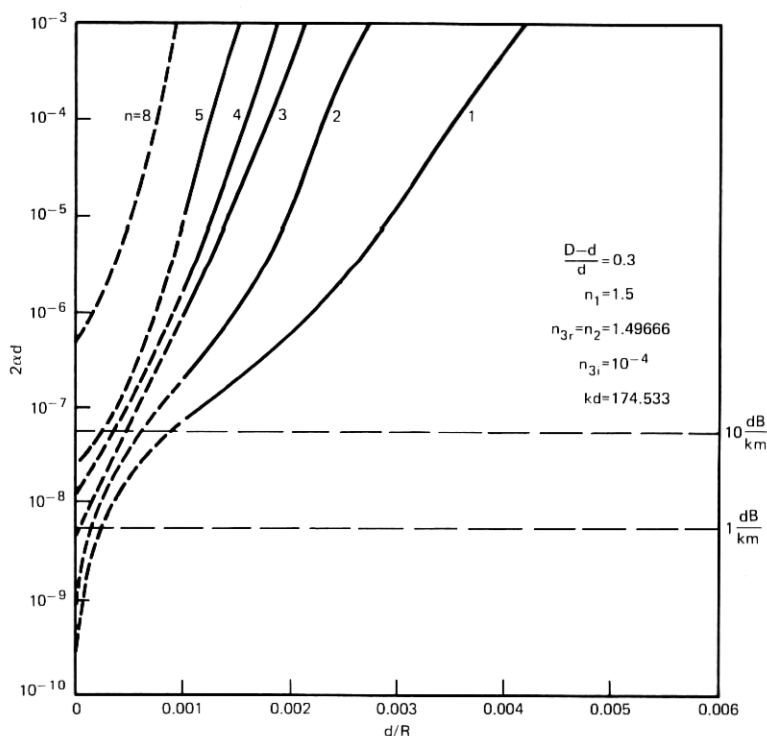


Fig. 7—Curvature losses in the presence of a lossy jacket. The normalized cladding thickness is  $(D - d)/d = 0.3$  and the refractive indices are  $n_1 = 1.5$ ,  $n_2 = 1.49666$ ,  $kd = 174.533$ ,  $n_{3r} = n_2$ ,  $n_{3i} = 10^{-4}$ .

core thickness is  $D - d = 0.3d$ . For  $D - d = 0.5d$ , we see from Fig. 5 that more than half the fiber modes would suffer losses in excess of 10 dB/km even in the straight guide. This estimate is based on a jacket with large refractive index,  $n_{3r} = n_1$ . For jackets with lower index, the losses would be reduced. But to be on the safe side, it seems advisable to design a jacket so that it does not cause excessive loss even in the worst possible case. The conditions corresponding to Fig. 6 show that well over half the fiber modes are transmitted with low loss as long as  $d/R < 0.0004$ .

Figures 7 through 9 apply to the case of a jacket with a refractive index whose real part is matched to the cladding,  $n_{3r} = n_2 = 1.49666$ . The imaginary part of the jacket index is  $n_{3i} = 0.0001$ . This modest value of the imaginary part of the refractive index results in a plane

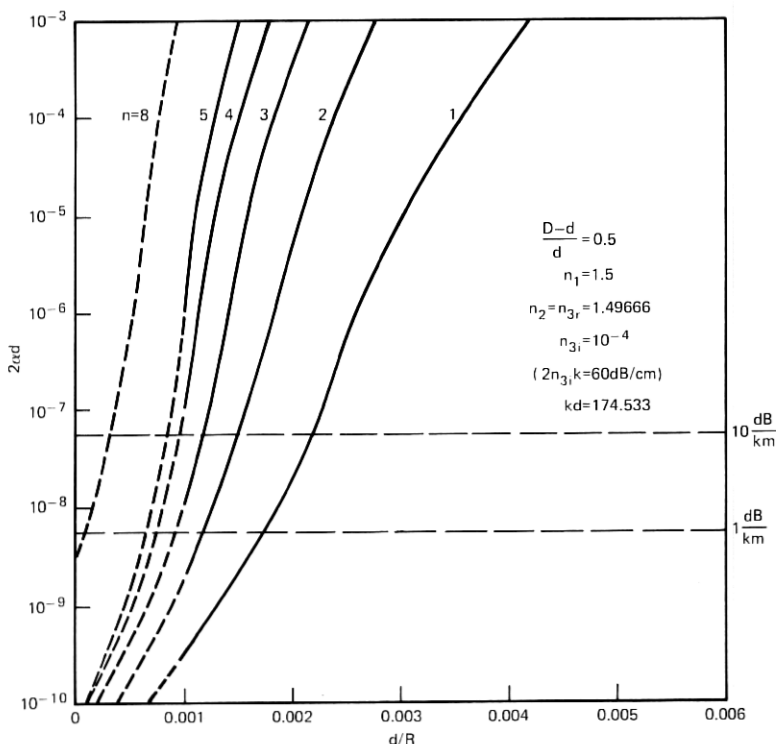


Fig. 8—Curvature losses in the presence of a lossy jacket. The normalized cladding thickness is  $(D - d)/d = 0.5$  and the refractive indices are  $n_1 = 1.5$ ,  $n_2 = 1.49666$ ,  $kd = 174.533$ ,  $n_{3r} = n_2$ ,  $n_{3i} = 10^{-4}$ .

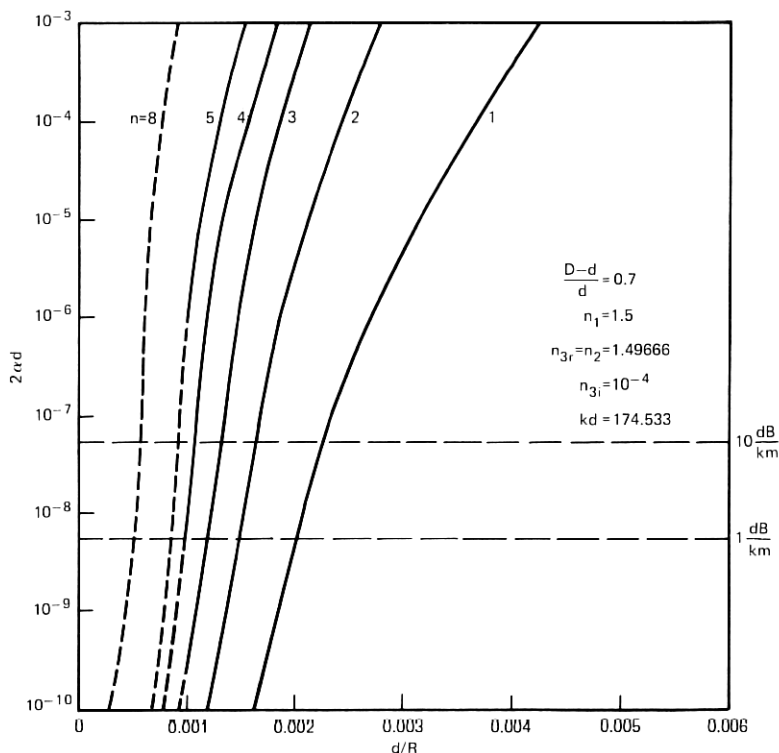


Fig. 9—Curvature losses in the presence of a lossy jacket. The normalized cladding thickness is  $(D - d)/d = 0.7$  and the refractive indices are  $n_1 = 1.5$ ,  $n_2 = 1.49666$ ,  $kd = 174.533$ ,  $n_{3r} = n_2$ ,  $n_{3i} = 10^{-4}$ .

wave loss in the jacket material that is given by

$$2\alpha_{\text{jacket}}d = 2n_{3i}kd. \quad (38)$$

For our particular example, we have  $2\alpha_{\text{jacket}}d = 0.035$ . For  $d = 25 \mu\text{m}$ , this cladding loss amounts to 61 dB/cm.

Comparison of Figs. 7 through 9 with Fig. 3 for the case of the infinitely thick cladding shows that the lossy jacket has a considerable influence if it is located too close to the waveguide core. However, even for  $(D - d)/d = 0.5$ , its influence on the curvature losses is only slight and all but vanishes for  $(D - d)/d = 0.7$ .

A lossy jacket with  $n_{3r} < n_2$  has only a very slight influence on the waveguide losses, since the evanescent field tail decays even more

rapidly in a medium of low refractive index. Therefore, no curves are provided for this case.

Figures 10 and 11 show the influence of the imaginary part of the refractive index of the jacket on the curvature losses. Figure 10 applies to the lowest-order mode,  $n = 1$ , and shows the dependence of the curvature loss on the logarithm of  $n_{3i}$  for  $R/d = 500$  and  $R/d = 1000$ . It is apparent that the dependence of the loss on  $n_{3i}$  is linear in regions of the curve that are dominated by the losses in the jacket. For very small values of  $n_{3i}$ , the losses of the jacket become immaterial and the curves approach asymptotically the curvature loss of a waveguide with lossless, infinitely thick cladding.

The two curves in Fig. 11 dramatize this behavior. For  $R/d = 1000$ , the losses of the third mode are still dominated by the loss of the

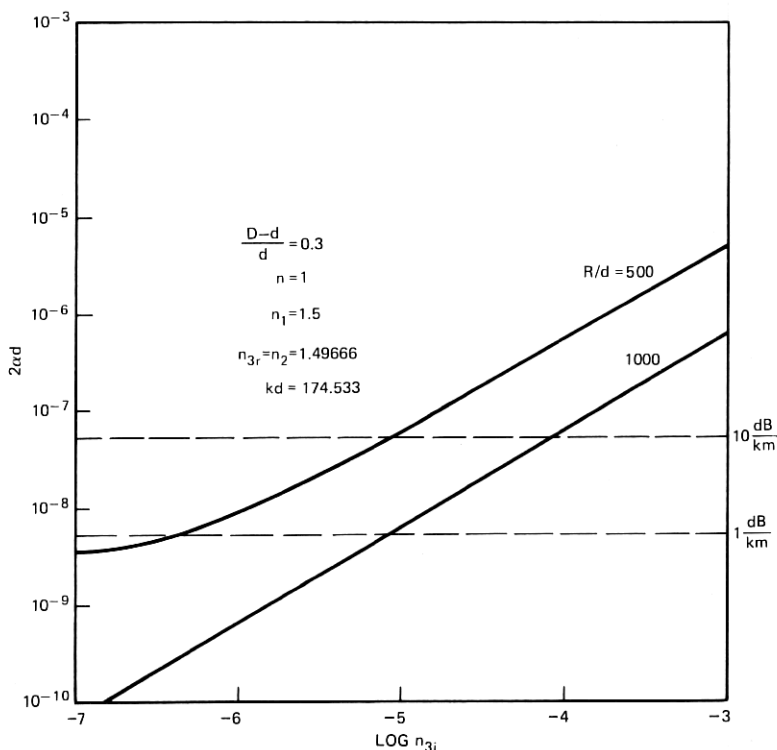


Fig. 10—Dependence of the curvature losses of the first mode on the imaginary part of the refractive index of the jacket material. The normalized cladding thickness is  $(D - d)/d = 0.3$  and the refractive indices are  $n_1 = 1.5$ ,  $n_2 = 1.49666$ ,  $kd = 174.533$ ,  $n_{3r} = n_2$ .

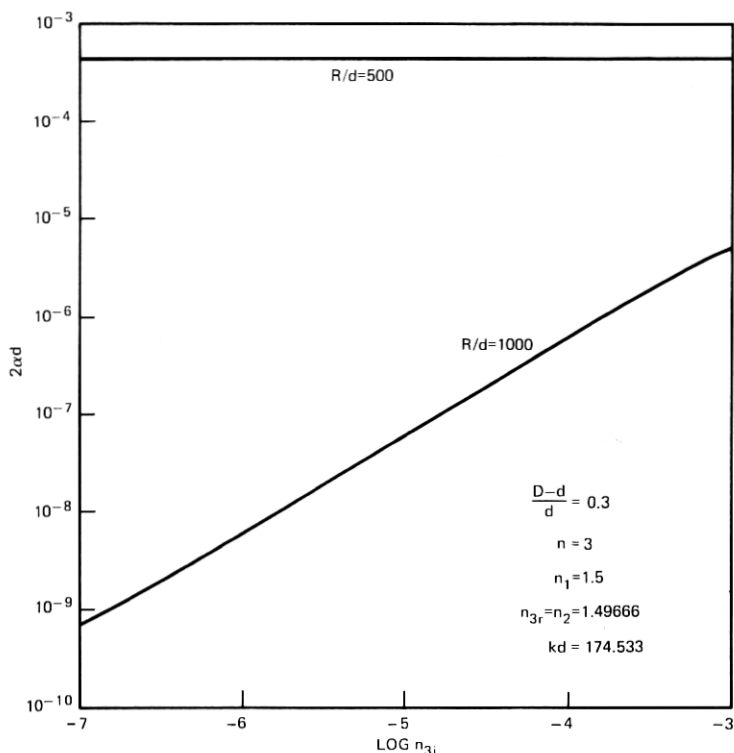


Fig. 11—Dependence of the curvature losses of the third mode on the imaginary part of the refractive index of the jacket material. The waveguide parameters are the same as in Fig. 10.

jacket. For  $R/d = 500$ , the field already radiates away in the space between core and jacket so that the losses are independent of the power dissipation in the jacket. Both figures are drawn for  $(D - d)/d = 0.3$ .

Finally, we discuss briefly a slab waveguide supporting  $N = 24$  TE modes. We use once more  $kd = 174.533$  and  $n_1 = 1.5$ , but choose the cladding index  $n_2 = 1.485$ . Figure 12 shows loss curves as functions of  $d/R$  for the mode  $n = 17$  for several values of the cladding thickness  $D - d$ . The jacket is of the "high-index" type, with  $n_{3r} = n_1$  since this condition results in high losses. Mode  $n = 17$  separates the corresponding modes of the fiber in equal halves. We see from Fig. 12 that even for a straight guide half the fiber modes have losses in excess of 5 dB/km if the cladding thickness is  $D - d = 0.3d$ . For  $D - d = 0.4d$ , the losses of the straight guide are reasonably low; they become im-

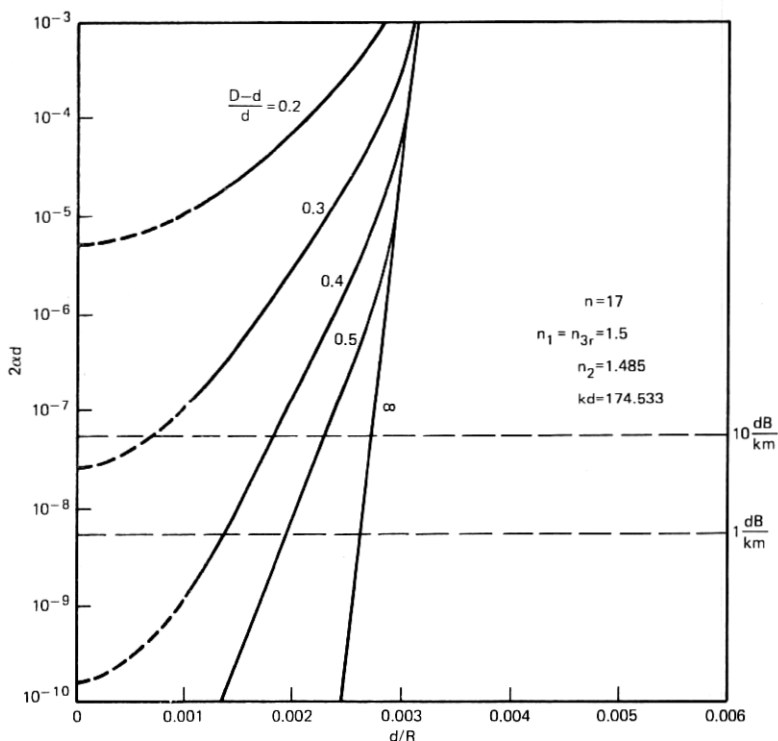


Fig. 12—Curvature losses in the presence of a jacket with  $n_{3r} = n_1$  for mode  $n = 17$  of a slab supporting 24 TE modes. The other parameters are  $n_1 = 1.5$ ,  $n_2 = 1.485$ ,  $kd = 174.533$ .

portant for  $d/R > 0.0015$ . The larger index difference of this example has the effect of allowing us to use a slightly thinner cladding and lower radii of curvature compared to the previous case with  $n_2 = 1.49666$ .

## VII. CONCLUSIONS

The presence of a jacket can increase the curvature losses of dielectric optical waveguide. It is thus important to keep the jacket sufficiently far from the waveguide core. The worst possible case is that of a jacket whose refractive index is slightly higher than the index of the cladding. However, we see an increase of the curvature losses caused by the power dissipation in the lossy jacket even if the real part of the index of the jacket is equal to the cladding index.

A first indication of trouble can be obtained by computing the losses caused by the presence of the jacket from formula (29) for a straight slab waveguide. (A corresponding formula for the  $HE_{in}$  modes of the round optical fiber can be found in eq. (10.4-22), p. 426, of Ref. 4.) Even if the presence of a lossy jacket does not seem to increase the losses of the straight guide above a certain tolerable level, it is important to keep in mind that waveguide curvature will increase the values of the loss coefficient by orders of magnitude for sufficiently tight bends.

The discussion of curvature losses in the presence of a lossy jacket was based on considering TE modes of a slab waveguide. The general behavior of the losses is expected to be the same for round optical fibers. Since experience has shown that even the numbers obtained from a slab model give the correct order of magnitude for round fibers, the numerical example discussed in this paper may be used to estimate the curvature losses of a round fiber with lossy jacket.

## REFERENCES

1. D. Marcuse, "Attenuation of Unwanted Cladding Modes," B.S.T.J., 50, No. 8 (October 1971), pp. 2565-2583.
2. E. A. J. Marcatili, "Bends in Optical Dielectric Waveguides," B.S.T.J., 48, No. 7 (September 1969), pp. 2103-2132.
3. M. A. Miller and V. I. Talanov, "Electromagnetic Surface Waves Guided by a Boundary with Small Curvature," Zh. Tekh. Fiz., 26, No. 12, 1956, p. 2755.
4. D. Marcuse, *Light Transmission Optics*, New York: Van Nostrand Reinhold, 1972, p. 290.
5. M. Abramovitz and I. A. Stegun, *Handbook of Mathematical Functions with Formulas, Graphs and Mathematical Tables*, National Bureau of Standards Applied Mathematics Series, Vol. 55, Washington D.C.: National Bureau of Standards, 1965.

